The Astrophysical Journal, 656:1092–1103, 2007 February 20

A FAR-ULTRAVIOLET STUDY OF THE NOVA-LIKE V794 AQUILAE[1]

Patrick Godon[2] and Edward M. Sion
Department of Astronomy and Astrophysics, Villanova University, Villanova, PA;
patrick.godon@villanova.edu, edward.sion@villanova.edu

Paul Barrett
United States Naval Observatory, Washington, DC; barrett.paul@usno.navy.mil

and

Paula Szkody
Department of Astronomy, University of Washington, Seattle, WA; szkody@astro.washington.edu
Received 2006 September 19; accepted 2006 November 8

ABSTRACT

V794 Aql was observed in a high state with the *Hubble Space Telescope* Space Telescope Imaging Spectrograph (*HST* STIS) on 2003 August 28, and with the *Far Ultraviolet Spectroscopic Explorer* (*FUSE*) on 2004 May 13. We present here a spectral analysis of the *FUSE* and *HST* STIS spectra. For a $0.9\,M_{\odot}$, the best fit is an accretion disk with a mass accretion rate $\dot{M} = 10^{-8.5}$ to $10^{-8.0}\,M_{\odot}\,\mathrm{yr}^{-1}$ with an inclination of 60° when assuming $E(B-V) = 0.2$. The corresponding distance to the system is $d = 690$ pc. A single white dwarf model leads to a rather hot temperature (between 30,000 and 55,000 K depending on the assumptions) but does not provide a fit as good as the accretion disk model. The same disk model is the best fit to the *FUSE* spectrum, the *HST* STIS spectrum, and the combined *FUSE* + *HST* STIS spectrum, implying therefore that the disk model is the best fit not only in the least χ^2 sense, but also as a consistent solution across a large-wavelength span of observation. We find that the model fits are in much better agreement with the dereddened spectra when $E(B-V)$ is large, as excess emission in the longer wavelengths renders the slope of the observed spectra almost impossible to fit, unless $E(B-V) = 0.2$. A large reddening value is in agreement with the hydrogen column density we find, $N(\mathrm{H\ I}) = 4.5 \times 10^{20}\ \mathrm{cm}^{-2}$ and $N(\mathrm{H_2}) = 3 \times 10^{17}\ \mathrm{cm}^{-2}$ and with the $E(B-V)$ value derived from the existing archival *International Ultraviolet Explorer* spectra.

Subject headings: accretion, accretion disks — novae, cataclysmic variables — stars: individual (V794 Aquilae) — ultraviolet: stars — white dwarfs

Online material: color figures

1. INTRODUCTION

Cataclysmic variables (CVs) are short-period, semidetached binary systems consisting of an accreting white dwarf (WD) star (the primary) and a low-mass main-sequence star (the secondary) as the Roche lobe–filling mass donor (Warner 1995). In nonmagnetic CV systems, the mass is accreted by means of an accretion disk reaching all the way down to the surface of the WD. Ongoing accretion at a low rate (quiescence) is interrupted every few weeks to months by intense accretion (outburst) of days to weeks—a dwarf nova (DN) accretion event. CV systems are divided in subclasses according to the durations, occurrence, and amplitude of their outburst: e.g., DN systems spend most of their time in the quiescent state, while nova-like (NL) systems are found mostly in the high outburst state. Both DN and nonmagnetic NL systems exhibit emission from the accretion disk during the high state.

Far-ultraviolet (FUV) observations have shown that some WDs in CVs can be directly viewed in the UV when the accretion disk is not dominant (as early as Mateo & Szkody [1984]). Consequently, much effort has gone into observing the systems with low mass transfer rates. In those systems the WDs are hotter than single field WDs and their temperature increases with orbital period, as higher accretion rates are found in longer period systems (Sion 1999). Interestingly enough, while the binary period of the CV systems ranges between a fraction of an hour (e.g., AM CVn systems) up to ≈2 days (e.g., GK Per), there is a gap between about 2 and 3 hr where almost no system is found (hereafter the "period gap"). However, at a given orbital period the accretion rate can vary by a large amount, and, unfortunately, for long period systems above the period gap ($P > 3$ hr) there are not many data points in the $T-P$ (temperature vs. orbital period) parameter space. In the accretion disk limit cycle (Cannizzo 1993), material accumulates in the accretion disk during quiescence and accretes onto the WD during outburst. In order for an outburst to occur, the accretion rate must be below a critical value for a given orbital period. Dwarf novae at periods above the gap should have accretion rates below the limit, the rates for Z Cam are very close to the critical value and the NL systems have rates above the limit. Thus, above the period gap, one finds three classes of systems: the U Gem (DN) type, which undergo outbursts; the Z Cam (DN) type, which have standstills where they remain at about 1 mag below their outburst level for long times (e.g., up to 50 days for AT Cnc; Shafter et al. 2005); and NL systems that are in a permanent high state.

Among the NL systems, the VY Sculptoris systems form a rather poorly understood subclass. VY Scl stars are apparently all disk systems with negligible (magnetic) accretion at the poles, and they fall just above the period gap, all in the range of 3–4 hr,

[1] Based on observations made with the NASA-CNES-CSA *Far Ultraviolet Spectroscopic Explorer*. *FUSE* is operated for NASA by The Johns Hopkins University under NASA contract NAS5-32985.

[2] Visiting at the Space Telescope Science Institute, Baltimore, MD; godon@stsci.edu.

Report Documentation Page

Form Approved
OMB No. 0704-0188

1. REPORT DATE	2. REPORT TYPE	3. DATES COVERED
20 FEB 2007		**00-00-2007 to 00-00-2007**

4. TITLE AND SUBTITLE	5a. CONTRACT NUMBER
A Far-Ultraviolet Study of the Nova-Like V794 Aquilae	5b. GRANT NUMBER
	5c. PROGRAM ELEMENT NUMBER
6. AUTHOR(S)	5d. PROJECT NUMBER
	5e. TASK NUMBER
	5f. WORK UNIT NUMBER
7. PERFORMING ORGANIZATION NAME(S) AND ADDRESS(ES) **United States Naval Observatory,Washington,DC**	8. PERFORMING ORGANIZATION REPORT NUMBER
9. SPONSORING/MONITORING AGENCY NAME(S) AND ADDRESS(ES)	10. SPONSOR/MONITOR'S ACRONYM(S)
	11. SPONSOR/MONITOR'S REPORT NUMBER(S)

12. DISTRIBUTION/AVAILABILITY STATEMENT
Approved for public release; distribution unlimited

13. SUPPLEMENTARY NOTES

14. ABSTRACT

15. SUBJECT TERMS

16. SECURITY CLASSIFICATION OF:			17. LIMITATION OF ABSTRACT	18. NUMBER OF PAGES	19a. NAME OF RESPONSIBLE PERSON
a. REPORT **unclassified**	b. ABSTRACT **unclassified**	c. THIS PAGE **unclassified**	**Same as Report (SAR)**	**12**	

TABLE 1
V794 Aql System Parameters

Parameter	Value
Subtype	VY Sculptoris
P_{orb} (d)	0.1533[a]
Inclination i (deg)	39 ± 17
M_1 ($M_\odot$)	0.88 ± 0.39
V_{max}	14.0
V_{min}	20.2[b]

[a] Honeycutt & Robertson (1998).
[b] The visual magnitude of V794 Aql usually ranges between ≈14 and 18 (Honeycutt & Robertson 1998), but it has also been observed in an extremely low state where the magnitude drops to ≈20 (Honeycutt & Schlegel 1985).

except for V751 Cyg with $P_{orb} > 4$ hr. While NL systems are characterized by an approximately steady, high rate of mass transfer (and consequently a high luminous accretion disk—a permanent high state), the VY Scl systems unpredictably go into low brightness states of little or no accretion when the disk greatly shrinks or vanishes and the underlying accretion heated hot WD is exposed. As a consequence, among the high-accretion NL systems, only the underlying WDs of three VY Scl systems (DW UMa [Knigge et al. 2000], TT Ari [Gänsicke et al. 1999], and MV Lyr [Hoard et al. 2004]) have been studied in the low state for temperature, gravity, rotation and chemical abundances information. All the other NL systems that have been observed have been caught in a high state. The spectra of NL systems (in permanent high state) consist of H emission lines, which may or may not be superimposed on broad shallow absorption features; the brightness fluctuates about some mean value, deviating up and down irregularly by no more than about 1 mag. The spectra in the near UV and optical are consistent with that of an accretion disk in outburst.

V794 Aql is a NL system belonging to the VY Sculptoris class, or at least it appears to have observational properties consistent with this class.

1.1. *V794 Aql*

The VY Scl systems all have extreme (3 mag) brightness variations in the high state and unexpectedly fall to an extreme low state (more than 5 mag). V794 Aql has been seen to vary erratically between photographic magnitudes 14 and 17 on timescales of days to years (Szkody et al. 1981), and Honeycutt & Schlegel (1985) observed V794 Aql in an unprecedented low state with magnitude 20! Photometrically speaking, V794 Aql seems to be one of the most active cataclysmic variables with brightness variations of up to 0.5 mag occurring on a timescale of minutes (and smaller flares on timescales of tens of seconds; Warner 1982). The brightness variations in VY Scl systems appear to be random in amplitude, shape, and recurrence interval. However, V794 Aql is an exception: photometric monitoring of V794 Aql has revealed an unusual type of light curve (Honeycutt et al. 1994; Honeycutt & Robertson 1998), in which the uniform decline from high to low state is interrupted by an abrupt return to the high state, giving the light curve a distinctive "sawtooth" appearance. This is a type of photometric variation in CVs which is unique to this system. V794 Aql is among the most puzzling of the VY Scl stars. The system parameters of V794 Aql are listed in Table 1.

V794 Aql was spectroscopically observed in high and low state in the optical (Szkody et al. 1981; Honeycutt & Schlegel 1985; Honeycutt & Robertson 1998), in the UV with *IUE* (Szkody et al. 1988; La Dous 1991) and in the X-ray with *Einstein* (Szkody et al. 1988), and, in respects other than the character of its long-term light curve, V794 Aql was found to have a photometric and spectroscopic behavior very similar to other members of the NL VY Sculptoris class, such as MV Lyrae and TT Arietis.

In the X-ray, V794 Aql was observed near a high state in terms of its optical range. The system had a flux of 4.5×10^{-12} ergs cm^{-2} s^{-1} (in the 0.1–4.5 keV band), corresponding to an X-ray luminosity of $L_X = 5.4 \times 10^{30}$ergs s^{-1}, for a distance $d = 100$ pc. The source was detected in both the soft (0.1–0.5 keV) and hard (0.5–4.5 keV) energy bands, and the hardness ratio was found to be 11 ± 2 (although the apparent hardness can be affected by the absorption of soft X-rays either at the source itself or in the interstellar medium [ISM], and ISM absorption might not be negligible for V794 Aql; see § 2.3). Simultaneous ground-based optical observations showed blue colors, strong H emission with a flat Balmer decrement, plus strong He I and He II λ4686 emission. These *IUE*, X-ray, and optical spectra show relatively strong emission lines of intermediate excitation, similar to those seen in other VY Sculptoris stars in both the low state and the high state. In the low state reported by Honeycutt & Schlegel (1985) the accretion disk emission lines were replaced by very narrow Balmer emission, in a behavior similar to (but more extreme than) that of MV Lyr (e.g., Hoard et al. 2004) and a few other NL systems in which the accretion apparently switches off for brief periods of time.

Although V794 Aql has many of the properties of a typical disk VY Scl star, there has been no direct evidence yet that a disk exists in this system. V794 Aql cannot be classified as a Z Cam system, as the sawtooths are consistently much fainter than the occasional intervals of steady brightness characteristic of Z Cam systems. If V794 Aql is a Z Cam system, then it is certainly a very unusual one.

Szkody et al. (1988) studied V794 Aql from *IUE* spectra; however, the low resolution and geocoronal contamination of the *IUE* spectra prevented accurate determination of the temperature and the low response shortward of Lyα prevented any observation of a rising continuum from the hot WD. This study estimated a white dwarf temperature near 50,000 K, while the accretion rate has been estimated to be around $10^{-8}\,M_\odot$ yr^{-1} (Honeycutt et al. 1994)-based on the long-term optical variations of the system. This NL system has the highest known mass accretion rate, above the limit for outbursts. Because of its inclination, both the hot WD and the inner disk might be observable.

More recently an *HST* STIS snapshot of V794 Aql was obtained, and the system was also observed in the FUV with *FUSE* under a Cycle 4 program. In this paper we report a spectral analysis of the *FUSE* and *HST*/STIS spectra of V794 Aql using accretion disk models, photosphere models, and models combining white dwarfs and accretion disks. Our objectives are to identify the source(s) of the FUV radiation, derive the properties of the WD (if possible), the accretion disk, and characterize the hot component in the system.

2. THE OBSERVATIONS

We report here all the ultraviolet spectra of V794 Aql. This includes five *IUE* archival spectra, one *HST* STIS spectrum, and one *FUSE* spectrum. While we model mainly the *FUSE* and *HST* STIS spectra, we also use the *IUE* spectra for flux comparison to estimate the relative state in which the system was found during each observation. For all the spectra we identify the emission and absorption features with a particular emphasis on the estimate of the molecular and atomic hydrogen column densities using the *FUSE* and *HST* STIS spectra (which covers the Lyα region). We use the

TABLE 2
OBSERVING LOG FOR V794 AQL

Telescope	Data Set	Date	t_{exp} (s)	Aperture	Additional Characteristics
IUE	SWP 15266	1981 Oct 14	7200	Large	Dispersion = low, continuum = 54 counts s^{-1}, background = 28 counts s^{-1}
	SWP 28501	1986 Jun 16	23400	Large	Dispersion = low, continuum = 118 counts s^{-1}, background = 73 counts s^{-1}
	SWP 50754	1994 May 13	7198	Large	Dispersion = low, continuum = 166 counts s^{-1}, background = 96 counts s^{-1}
	SWP 14708[a]	1981 Aug 10	3600	Large	Dispersion = low, continuum = 0 counts s^{-1}, background = 23 counts s^{-1}
	LWR 11782	1981 Oct 15	3600	Large	Dispersion = low, continuum = 72 counts s^{-1}, background = 34 counts s^{-1}
FUSE	D1440101	2004 May 13	13,333	LWRS	Mode = TTAG, central wavelength = 959.998 Å
HST STIS	O8MZ66010	2003 Aug 28	830	0.2 × 0.2	Mode = ACCUM, filter/grating = G140L

[1] SWP 14708 has a flux level of the order of 10^{-15} ergs s^{-1} cm^{-2} $Å^{-1}$ and cannot be used.

IUE spectra to carry out an assessment of the reddening of the system. The reason for questioning the zero color excess value of Verbunt (1987) is in part the a posteriori fact that the slope of the continuum (both in the *FUSE* and STIS spectra) cannot be easily matched with the model fits when assuming a small $E(B-V)$ value. We obtain a large residual in the longer wavelength indicating a net excess of flux in the "red" part of the spectrum. This discrepancy basically disappears when we deredden the spectra assuming $E(B-V) = 0.2$. In addition, the hydrogen column density we obtain from the *FUSE* and STIS spectra leads to a reddening of $E(B-V) = 0.08$ using the relation of Bohlin et al. (1978).

2.1. *The IUE Archival Spectra*

The *IUE* archive contains three good observations of V794 Aql with the short-wavelength prime (SWP) camera through the large aperture at low dispersion (see Table 2 and Fig. 1). One additional *IUE* SWP spectrum (SWP 14708) has an extremely low flux level and a very low signal-to-noise ratio (S/N). This spectrum has been disregarded here as it has basically no continuum and cannot be used. The *IUE* SWP spectra have a wavelength binning of 1.68 Å, covering the wavelength range 1150–1980 Å. There is also a data set obtained with the long-wavelength camera, LWR 11782, which we use to assess the reddening of the system. The *IUE* LWR spectrum has a wavelength binning of 1.67 Å, and covers the wavelength range 1850–3350 Å. All the *IUE* NEWSIPS spectra were flux-calibration corrected using the Massa-Fitzpatrick corrections (Massa & Fitzpatrick 2000). These spectra were analyzed in detail by Szkody et al. (1988) and La Dous (1991).

The SWP 28501 spectrum was obtained when the system had a visual magnitude of 17–18, a relatively low state, although not the lowest state of V794 Aql (magnitude 20 reported by Honeycutt & Schlegel (1985)). The spectrum SWP 15266 has a flux only

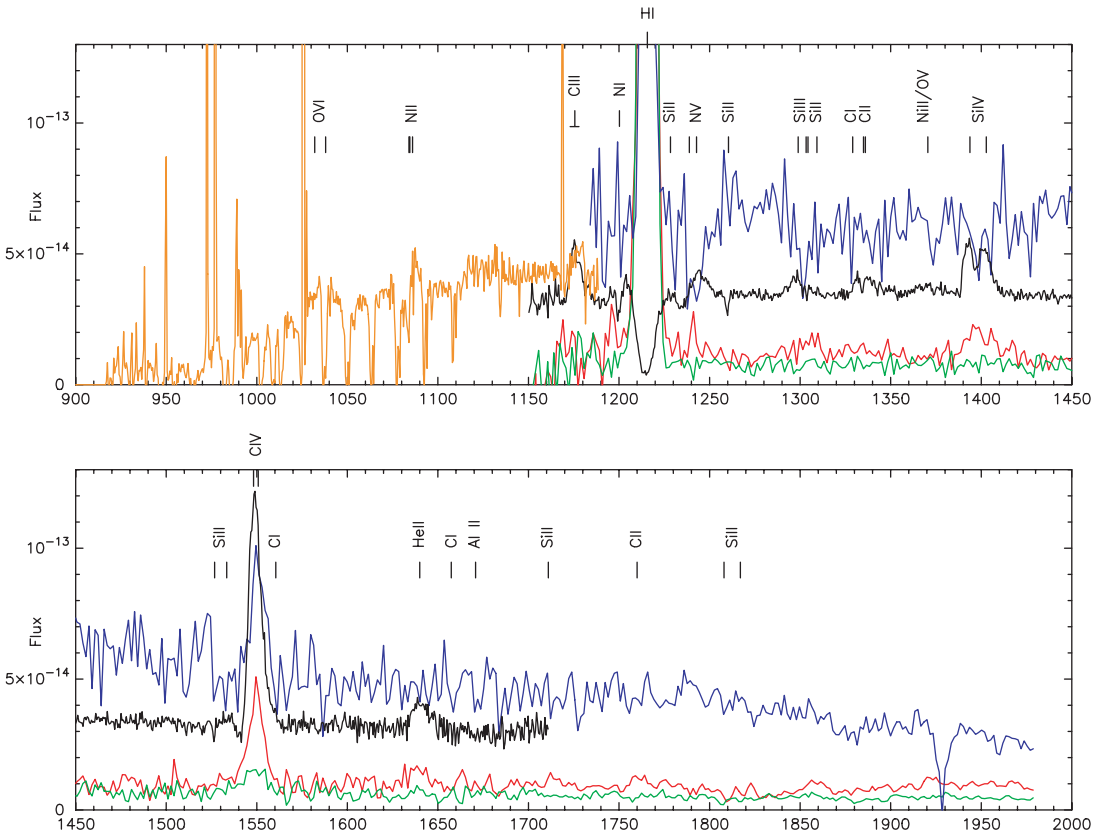

FIG. 1.—*FUSE*, *HST* STIS, and *IUE* spectra of V794 Aql with line identification in the STIS and *IUE* range. *FUSE* is in orange, STIS is in black, the *IUE* SWP 50754 is in blue, SWP 28501 is in red, and SWP 15266 is in green. The *FUSE* spectrum has been binned to 0.5 Å here. The flux (*y*-axis) is given in ergs s^{-1} cm^{-2} $Å^{-1}$, and the wavelength (*x*-axis) is given in Å. The sharp emission lines in the *FUSE* spectrum and the strong Lyα emission in the *IUE* spectra are all due to air glow. Line identification for *FUSE* is provided in Fig. 3 and Tables 3 and 4.

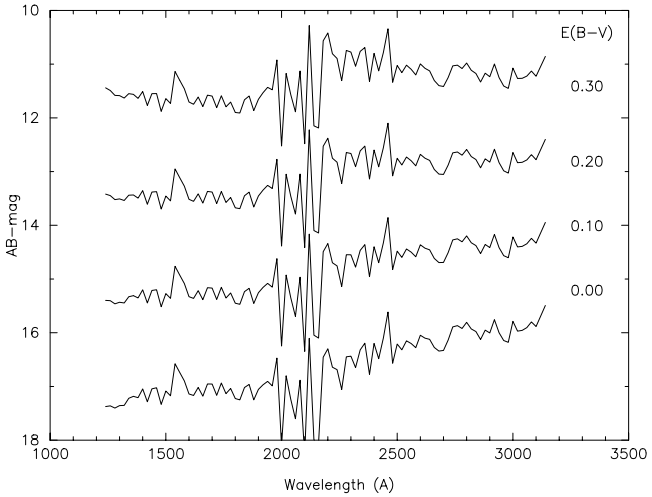

FIG. 2.—*IUE* SWP 28501 and LWR 11782 spectra of V794 Aql have been combined together and binned at 20 Å following the procedure of Verbunt (1987). The AB magnitude is shown as a function of wavelengths (Å) for the dereddened spectra assuming a different value of $E(B-V)$. The broad absorption feature between 2000–2400 Å is clearly seen in the lower graph, a sign that $E(B-V) > 0$.

slightly larger than SWP 28501, but in addition it exhibits some broad emission lines. The most prominent ones are N v (1238–1243 Å), Si iv (1394–1403 Å), C iv (1548–1550 Å), and He ii (1640 Å Balmer α). With its broad emission lines characteristic of NL systems, the spectrum of V794 Aql shows evidence of hot gas. The SWP 50754 shows the system in a relatively higher state with emission and absorption features; however, the S/N of this spectra is very low.

The presently accepted value for the reddening of V794 Aql is $E(B-V) = 0$ (e.g., La Dous [1991] and Bruch & Engel [1994], based on the work of Verbunt [1987]). However, the heavy interstellar hydrogen absorption in its *FUSE* spectrum (see next subsection) implies that the source is either located pretty far away, or masked by an ISM cloud, or some cold circumstellar matter, and consequently it is probably also affected by dust, therefore making the assumption $E(B-V) = 0$ very unlikely. In his pioneer work, Verbunt (1987) carried out an analysis of the broad (several hundreds Å) absorption feature around 2175 Å of the *IUE* spectra of 51 CV systems to determine their reddening value $E(B-V)$. The reddening of the 51 systems was assessed by dereddening each spectrum assuming increasing values of $E(B-V)$ (e.g., 0.05, 0.10, 0.15. . .) until the broad absorption dip (between ≈2000 and ≈2400 Å) disappeared completely to the "eye" [.e., the acceptable range of values of $E(B-V)$ were found by visual inspection].

Following Verbunt (1987), we first combine the *IUE* spectra SWP 28501 and LWR 11782 binned at 20 Å (we have chosen the SWP 28501 spectrum as it matches the flux level and shape of LWR 11782). The spectra are very noisy, including a "hot pixel" at 2200 Å. This combined spectrum is then dereddened assuming values $E(B-V) = 0.10$, 0.20, and 0.30. In Figure 2 we plot the AB magnitude (Oke 1974) for each dereddened spectrum for visual inspection. From Figure 2 we see that the dereddened spectrum that leaves neither excess emission nor absorption near the 2200 Å feature is for an extinction value $E(B-V) = 0.2$.

2.2. *The FUSE Observations*

FUSE is a low-earth orbit satellite, launched in 1999 June. Its optical system consists of four optical telescopes (mirrors), each separately connected to a different Rowland spectrograph. The four diffraction gratings of the four Rowland spectrographs produce four independent spectra on two microchannel plates. Two mirrors and two gratings are coated with SiC to provide wavelength coverage below 1020 Å, while the other two mirrors and gratings are coated with Al and LiF. The Al+LiF coating provides about twice the reflectivity of SiC at wavelengths >1050 Å, and very little reflectivity below 1020 Å (hereafter the SiC1, SiC2, LiF1, and LiF2 channels).

A TIME TAG *FUSE* spectrum (D1440101) of V794 Aql was obtained starting on 2003 May 13, (at 19 : 50:22) with a total observing duration covering six individual spacecraft orbits through the LWRS aperture. The system was in a relatively high state at the time of the observation. The data were processed with CalFUSE version 3.0, totaling 13,066 s of good exposure time. The main change from previous versions of CalFUSE is that now the data are maintained as a photon list (the intermediate data file) throughout the pipeline. Bad photons are flagged but not discarded, so the user can examine, filter, and combine data without rerunning the pipeline. A number of design changes enable the new pipeline to run faster and use less disk space than before. Processing time with CalFUSE has decreased by a factor of up to 10. In this version, event bursts are automatically taken care of (see the *FUSE* Instrument and Data Handbook). Event bursts are short periods during an exposure when high count rates are registered on one of more detectors. The bursts exhibit a complex pattern on the detector, their cause, however, is yet unknown (it has been confirmed that they are not detector effects).

During the observations, Fine Error Sensor A, which images the LiF 1 aperture was used to guide the telescope. The spectral regions covered by the spectral channels overlap, and these overlap regions are then used to renormalize the spectra in the SiC1, LiF2, and SiC2 channels to the flux in the LiF1 channel. We then produced a final spectrum that covers almost the full *FUSE* wavelength range 905–1182 Å. The low-sensitivity portions of each channel were discarded. Here we took particular care to discard the portion of the spectrum where the so-called *worm* "crawls" (see the *FUSE* Instrument and Data Handbook and § 2.1 in Godon et al. [2006]), which deteriorates LiF1 longward of 1125 Å (CalFUSE cannot correct target fluxes for this effect). Because of this the 1182–1187 Å region was lost. We combined the individual exposures and channels to create a time-averaged spectrum with a linear, 0.1 Å dispersion, weighting the flux in each output datum by the exposure time and sensitivity of the input exposure and channel of origin.

V794 Aql, with a flux of a few 10^{-14} ergs s^{-1} cm^{-2} $Å^{-1}$, is actually a relatively weak source. The procedure we used to process the *FUSE* data of V794 Aql is the same as the one we used in our previous *FUSE* analysis of CVs, such as, e.g., RU Peg and SS Aur (Sion et al. 2004), VW Hyi (Godon et al. 2004), and WW Cet (Godon et al. 2006).

2.3. *Interstellar Absorption Toward V794 Aql*

A single look at the *FUSE* spectrum of V794 Aql (Fig. 3) immediately reveals that the continuum is moderately affected by hydrogen absorption: the continuum is basically sliced (at almost equal intervals) by interstellar hydrogen lines starting at wavelengths around 1110 Å and continuing toward shorter wavelengths all the way down to the hydrogen cut-off around 915 Å. In Table 3 we identified all the absorption and emission lines of metals in the *FUSE* spectrum of V794 Aql. In Table 3 we identified the most prominent molecular hydrogen absorption lines by their band (Werner or Lyman), upper vibrational level

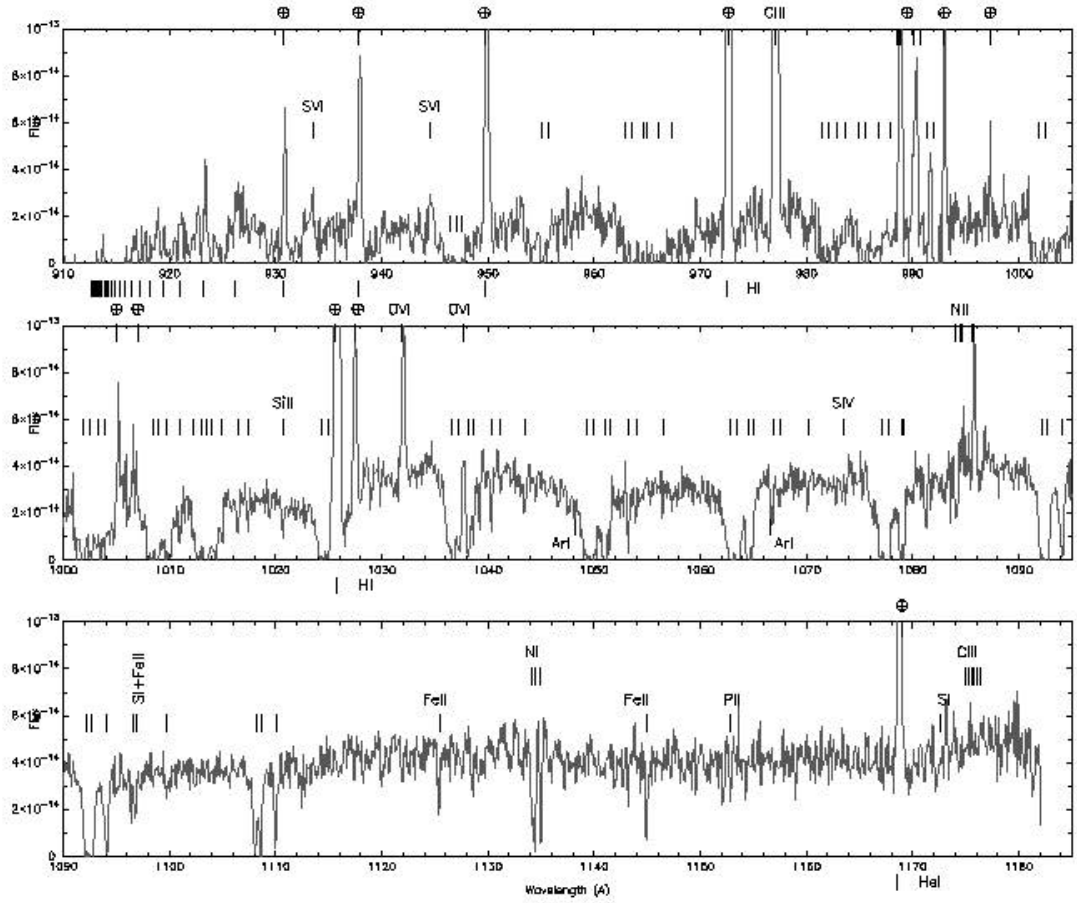

FIG. 3.—*FUSE* spectrum of V794 Aql with line identification. The flux (*y*-axis) is in ergs s^{-1} cm^{-2} $Å^{-1}$ and the wavelength (*x*-axis) is in Å. The airglow (sharp) emission lines have been annotated with a circle with a cross; on top of the O VI and C III (λ977) broad emission from the source, there is a contribution from heliocoronal emission. The helium and hydrogen emission from the airglow have been annotated under the *x*-axis for clarity. The short vertical lines without annotation are the molecular hydrogen absorption lines due to the ISM. The nitrogen I and II are contaminated with airglow and ISM absorption lines. The spectrum here has not yet been dereddened. [*See the electronic edition of the Journal for a color version of this figure.*]

(1-16), and rotational transition (*R*, *P*, or *Q*) with lower rotational state ($J = 1, 2, 3$).

Next, we model the ISM hydrogen absorption lines to assess the atomic and molecular column densities. We use a custom spectral fitting package to estimate the temperature and density of the interstellar absorption lines of atomic and molecular hydrogen. The ISM model assumes that the temperature, bulk velocity, and turbulent velocity of the medium are the same for all atomic and molecular species, whereas the densities of atomic and molecular hydrogen, and the ratios of deuterium to hydrogen and metals (including helium) to hydrogen can be adjusted independently. The model uses atomic data of Morton (2000, 2003) and molecular data of Abgrall et al. (2000). The optical depth calculations of molecular hydrogen have been checked against those of McCandliss (2003).

For V794 Aql, the ratios of metals to hydrogen and deuterium to hydrogen are fixed at 0 and 2×10^{-5}, respectively, because of the low S/N data. The wings of the atomic lines are used to estimate the density of atomic hydrogen and the depth of the unsaturated molecular lines for molecular hydrogen. The temperature and turbulent velocity of the medium are primarily determined from the lines of molecular hydrogen when the ISM temperatures are <250 K.

In order to model the atomic hydrogen column density correctly, we take care to include the portion of the *HST* STIS spectrum exhibiting the Lyα feature into the modeling. The ISM absorption features are best modeled and displayed when the theoretical ISM model (transmission values) is combined with a synthetic spectrum for the object (namely, a WD or an accretion disk spectrum; see § 3.2 for the spectral modeling of the WD and the accretion disk). In Figure 4 we show our fit to the (atomic and molecular) hydrogen absorption lines to the *FUSE* spectrum of V794 Aql, as applied to our accretion disk model fit. Namely, we multiplied the accretion disk synthetic spectral model by the transmission values of the ISM model. This ISM model has zero metallicity, a temperature of 150 K, a turbulent velocity of 40 km s^{-1}, a molecular hydrogen column density of 3×10^{17} cm^{-2}, and an atomic hydrogen column density of 4.5×10^{20} cm^{-2}. The Lyβ feature around 1025 Å is obviously far too sharp to be due to the disk; even with an inclination of only 20° this feature would be much broader. This absorption feature cannot be accounted for by the star itself either and it is modeled here as part of the ISM model.

It is interesting to note that the hydrogen column density of V794 Aql that we obtain here is very similar to the hydrogen column density of V1432 Aql (Rana et al. 2005), which is located in the same region of the sky (at about 230 pc). V1432 Aql is much closer to V794 Aql than any of the nearest neighboring sources found by the ISM hydrogen column density tool from the *EUVE* World Wide Web site. Also in the same vicinity and at about the

TABLE 3
FUSE Lines

Line Identification	Wavelength (Å)	Absorption/Emission[a]	Origin[b]
S VI	944.50	E	S
	933.50	E	S
N I	964.63	A	ISM
C III	977.02	E	C, S
Si II	1020.70	A	ISM, S
O VI	1031.93	E	C, S
	1037.62	E	C, S
Ar I	1048.20	A	ISM
	1066.66	A	ISM
S IV	1073.52	A	S
N II	1083.99	A, E	C, ISM
	1084.56	A, E	C, ISM
	1084.58	A, E	C, ISM
	1085.53	A, E	C, ISM
	1085.55	A, E	C, ISM
	1085.70	A, E	C, ISM
S I	1096.60	A	S
Fe II	1096.88	A	ISM
Fe II	1125.45	A	ISM
N I	1134.16	A	ISM
	1134.42	A	ISM
	1134.98	A	ISM
Fe II	1144.94	A	ISM
P II	1152.82	A	ISM
He I	1168.61	E	C
S I	1172.55	A	S

[a] E = emission, A = absorption.
[b] C = contaminated by airglow or geocoronal or heliocoronal emission; S = system; and ISM = interstellar medium The contamination is from geocoronal lines mainly: H I, O I, N I, and N II, and scattered solar light, such as the sharp C III (977 Å) and O VI (1032 Å), which are mainly seen here in the SiC channels.

TABLE 4
Molecular Hydrogen Absorption Lines

Line Identification	Wavelength (Å)	Line Identification	Wavelength (Å)
H_2 blend	946–948	L6R1	1024.99
L13R1	955.06	L5R0	1036.55
L13P1	955.71	L5R1	1037.15
L12R0	962.98	L5P1	1038.16
L12R1	963.61	L5R2	1038.69
H_2 blend	965.00	L5P2	1040.37
W2Q1	966.09	L5R3	1041.16
W2Q2	967.28	L5P3	1043.50
L10R0	981.44	L4R0	1049.37
L10R1	982.07	L4R1	1049.96
L10P1	982.84	L4P1	1051.03
L10R2	983.59	L4R2	1051.50
L10P2	984.86	L4P2	1053.28
W1R0+W1R1	985.60	L4R3	1053.98
W1R1	986.80	L4P3	1056.47
W1R2	987.97	L3R0	1062.88
L9R0	991.38	L3R1	1063.46
L9R1	992.01	L3P1	1064.61
L8R0	1001.82	L3R2	1065.00
L8R1	1002.45	L3P2	1066.90
L8P1	1003.29	L3R3	1067.48
L8R2	1003.98	L3P3	1070.14
W0R0+W0R1	1008.50	L2R0	1077.14
W0R2	1009.02	L2R1	1077.70
W0R1	1009.77	L2P1	1078.93
W0R2	1010.94	L2R2	1079.23
W0P2	1012.17	L1R0	1092.20
L7R0	1012.70	L1R1	1092.73
L7R1	1013.44	L1P1	1094.05
L7P1+W0P3	1014.50	L1P3	1099.79
L7R2	1014.97	L0R0	1108.13
L7P2	1016.46	L0R1	1108.63
L7R3	1017.42	L0P1	1110.06
L6R0	1024.37	L0R2	1110.12

same distance (250 ± 100 pc), UU Aql exhibits strong hydrogen absorption features in it *FUSE* spectrum (Sion et al. 2007). This seems to indicate that this region of sky in the constellation of Aquila might have an ISM cloud in the foreground (say at $d < 200$ pc or less).

Next, we use the hydrogen column density we obtained to estimate the reddening of the system using the analytical expression given by Bohlin et al. (1978):

$$E(B-V) = \frac{N(\mathrm{H\ I} + \mathrm{H_2})}{5.8 \times 10^{21}\ \mathrm{atoms\ cm^{-2}\ mag^{-1}}}. \quad (1)$$

Using our computed ISM value for the hydrogen column density $N(\mathrm{H_2}) = 3 \times 10^{17}$ cm^{-2} and $N(\mathrm{H\ I}) = 4.5 \times 10^{20}$ cm^{-2} in equation (1), we obtain $E(B-V) = 0.08$. The actual reddening toward V794 Aql could be smaller or larger than 0.08. Taking into consideration the results from § 2.1 (Fig. 2), we decide in the present work to model the spectra of V794 Aql for two values of the reddening, namely, $E(B-V) = 0.1$ and $E(B-V) = 0.2$.

2.4. *The HST STIS Spectrum*

An *HST* STIS snapshot spectrum of V794 Aql was obtained on August 28 2003, totaling 830 s of exposure time. The spectrum was taken with the 0.2×0.2 aperture in ACCUM (accumulation) mode using the G140L grating, covering the wavelength range from 1150 to 1710 Å, with a wavelength binning of ≈0.6 Å. The use of G140L provides a higher resolution spectrum than *IUE*, but not as high as when using E140M. The spectrum was taken in a relatively high state, similar to the state during which the *FUSE* spectrum was obtained. The spectrum exhibits some broad emission lines, mainly C III (1175 Å), N V (1240 Å), Si IV (1400 Å), C IV (1550 Å), and He II (1640 Å). Other possible lines are also annotated in Figure 1. Also very pronounced is the Lyα absorption feature (around 1215 Å). On the sides of the Lyα absorption feature there is some emission from N II on the left and Si II on the right. The Lyα absorption feature is too sharp to be that of the WD and/or the accretion disk of V794 Aql; however, it agrees very well with the hydrogen column density we found, except that it should be saturated, as the transmission values of the ISM model are null there due the high column density of atomic hydrogen. The only reason the Lyα is not saturated in the observed STIS spectrum of V794 Aql is because the spectral resolution ($2 \times 0.6 = 1.2$ Å) of the G140L grating combined with the short exposures required by snapshots often does not resolve the sharp geocoronal H I emission, seen in many STIS G140L exposures of some systems. For example the (MAST) archived STIS snapshot of VY Scl [with $E(B-V) = 0.06$; Bruch & Engel 1994] has a sharp Lyα absorption feature that is not saturated, and the STIS snapshots of SS Aur and V442 Cen [with $E(B-V) = 0.08$ and 0.15, respectively; Bruch & Engel 1994] show clearly a sharp emission peak in the bottom of their Lyα profile. All these systems with a reddening value as large as that of V794 Aql have most probably an atomic hydrogen column density larger than 10^{20} cm^{-2} and should therefore all have a saturated Lyα absorption feature

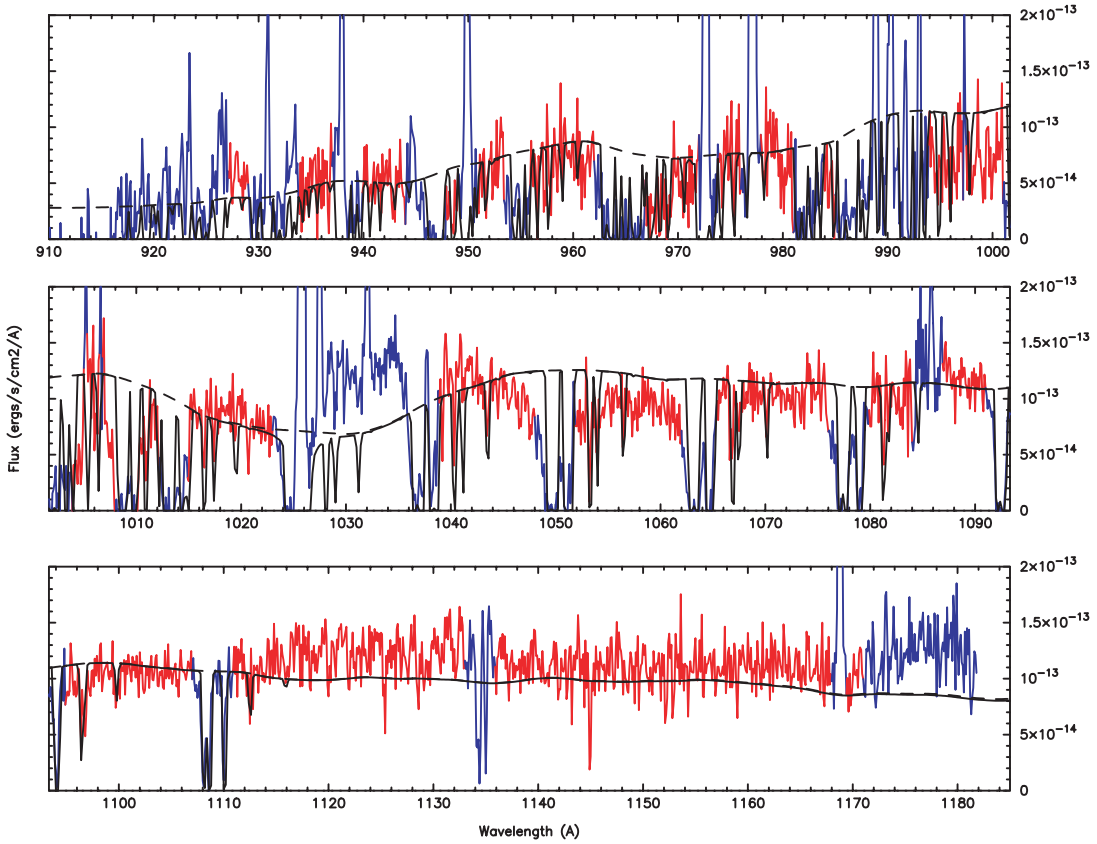

FIG. 4.—Best synthetic spectral fit (*solid black line*) using a disk model to the dereddened *FUSE* spectrum of V794 Aql (*in red and blue*) assuming $E(B-V) = 0.1$. Using the grid of models from Wade & Hubeny (1998), we find the best fit is for a WD with a mass $M = 1.03\ M_{\odot}$, a mass accretion rate $\dot{M} = 10^{-9.0}\ M_{\odot}\ \mathrm{yr}^{-1}$, an inclination of $i = 60^{\circ}$, and a distance of 616 pc. The resulting reduced χ^2 is $\chi^2_{\nu} = 0.02584$. The synthetic spectrum has been multiplied by the transmission values of the ISM model to match the ISM absorption feature. The strong emission lines (such as O VI and C III), the ISM absorption features, and the airglow lines have all been masked and are shown here in blue. The dotted line shows the synthetic spectrum without the ISM model. The fit is carried between the solid black line and the red portions of the observed spectrum.

(for any line of sight with $N(\mathrm{H\ I}) > 10^{14}\ \mathrm{cm}^{-2}$ the Lyα absorption feature should be saturated).

3. SYNTHETIC SPECTRAL MODELING

3.1. *Preparation of the Spectra*

Not enough light-curve data points were available from the American Association of Variable Star Observers (AAVSO) to determine whether V794 Aql was observed in a high or low state. However, a comparison of the *FUSE* spectrum with the *IUE* archival spectra and the *HST* STIS snapshot (see Fig. 1) helps us to assess the state in which the system was at the time each observation was made. From that figure it is clear that V794 Aql was observed in about four different states.

The lowest *IUE* spectrum has a flux about 5 times lower than the *FUSE* and STIS spectra. This *IUE* spectrum, however, was itself not obtained during the lowest state ($B = 20$). In the low state the contribution of the disk is negligible, and one expects to see WD; in the high state the accretion disk dominates and the WD contributes little to the flux (for large inclination systems the WD is totally masked by the accretion disk). It seems therefore quite clear that the *FUSE* and STIS spectra of V794 Aql need mainly to be modeled with a disk model and the contribution of the WD might be small. Although there is a large error bar on the mass of the WD ($0.88 \pm 0.4\ M_{\odot}$), we deliberately decided to use only one mass in our modeling ($M = 0.9\ M_{\odot}$) to limit the number of unknown parameters in the system: the distance, the inclination $i = 39^{\circ} \pm 17^{\circ}$, the reddening. We deredden the spectra assuming a reddening of $E(B-V) = 0.1$ and 0.2.

We prepared the *FUSE* and *HST* spectra for fitting by masking regions containing emission lines and artifacts. These regions are emphasized with a blue color in Figures 4–9. These regions of the spectrum were not included in the fitting. A comparison of the *HST* STIS spectrum with the *FUSE* spectrum in the wavelength overlap region reveals that the flux levels match thus enabling us to carry out model fits over a substantially broader wavelength range.

3.2. *The Synthetic Spectra*

The high-gravity white dwarf atmosphere model spectra are generated assuming solar abundances (unless otherwise specified) using TLUSTY200 (Hubeny 1988), SYNSPEC48, and ROTIN4 (Hubeny & Lanz 1995). TLUSTY generates numerical models of stellar atmospheres for a given surface gravity and effective temperature. SYNSPEC is then used to generate a synthetic spectrum for each particular stellar atmosphere model. The routine ROTIN is used last to perform a rotational and/or instrumental convolution of the synthetic spectrum obtained from SYNSPEC. For the input temperature in TLUSTY, we chose T ranging from 15,000 to 55,000 K by increments of 5000 K at first, and when a best fit is found a refined fitting is carried out by changing the temperature in increments of 1000 K. We chose a value of $\log g$ to match the mass of the WD in V794 Aql, namely, $\log g = 8.5$. We also varied the stellar rotational velocity $V_{\mathrm{rot}} \sin i$ from 100 to

600 km s^{-1} in steps of 100 km s^{-1}. We have the possibility to change the abundance of elements; however, we first ran a model with solar composition and only changed the Si and C abundances in two cases, to assess how it affects the results.

For the synthetic accretion disk models, we used the latest accretion disk models from the optically thick disk model grid of Wade & Hubeny (1998). The accretion disk models depend on the gravity ($\log g$) of the accreting central star since g dictates the Keplerian rotation law in the disk. Therefore, the accretion disk models in the grid of Wade & Hubeny (1998) varies as follows: WD mass (in solar masses) values of 0.35, 0.55, 0.80, 1.03, and 1.21; orbital inclination (in degrees) of 18, 41, 60, 75, and 81. The accretion rate ranges from $10^{-10.5}$ to $10^{-8.0}\ M_\odot\ \mathrm{yr}^{-1}$, varying in increments of 0.5 in $\log \dot{M}$. For the present work we select from this grid the models with parameters consistent with Table 1, namely, WD masses 0.80 and 1.03 $M_\odot$, inclination angles of 18°, 41°, and 60°, and the entire range of mass accretion rates from the grid of Wade & Hubeny (1998).

For combined accretion disk and stellar WD atmosphere models, the disk flux is divided by 100 to normalize it at 1000 pc to match the WD flux, therefore giving explicitly the relative flux contributions of each component. Then both fluxes are added for comparison with the observed flux. The best two-component models are not necessarily a combination of the best WD models with the best disk models. The main aim here is to find a fit that is better (lower χ^2_ν) than either the WD model fit or the accretion disk model fit used alone.

Before finding the best fit, all the synthetic spectral models (WD, accretion disk, and WD + accretion disk) are multiplied by the transmission values of the ISM model presented in § 2.2.

3.3. *The χ^2 Minimization Routine and the Best Fit*

In order to find the best model, we use FIT—a χ^2 minimization routine (see, e.g., Press et al. 1992). For each model, we computed χ^2_ν and scale factor values; χ^2_ν is known as the "reduced" χ^2, namely, χ^2 per number of degrees of freedom. In the present case the number of degrees of freedom is the number of wavelength bins of the observed spectrum taken into account in the fitting. Therefore, when we exclude (i.e., mask) regions of the spectrum (such as broad emission lines and features such as air glow) in preparation for the fitting, we reduce the number of degrees of freedom. And when we merge the *FUSE* spectrum together with the *HST* STIS spectrum we actually increase the number of degrees of freedom. Since *FUSE* and STIS are binned differently and have different errors, one cannot compare least χ^2_ν obtained by fitting the *FUSE* spectrum alone with the least χ^2_ν obtained when fitting the STIS spectrum alone or the combined *FUSE*+STIS spectrum. These fits cannot be compared on the basis of their χ^2_ν values, as the same synthetic model will lead to different χ^2_ν values when fitting the *FUSE* spectrum alone, the STIS spectrum alone, or the combined *FUSE*+STIS spectrum. So the analysis of the *FUSE*, STIS, and the combined *FUSE*+STIS spectra are carried out separately.

For each single value of $\log g$ there exists only one value of R_{WD} and M_{WD}, since we use the mass radius relation for WDs (see, e.g., Hamada & Salpeter [1961] or Wood [1990] for different composition and non-zero-temperature WDs). As a consequence, when fitting the theoretical flux to the observed flux, the distance to the system is obtained as an output parameter when scaling the fluxes. When the WD mass and distance of a system are known, the fitting technique leads to only one precise value of the WD temperature. In the present case, since neither the mass nor the distance are known, the best-fit model consists actually of a whole domain in the $\log g$–T_{eff} plane. Because of that we fix the WD mass to 0.9 $M_\odot$ (for the WD models) and use the $M_{\mathrm{WD}} = 0.80$, 1.03 $M_\odot$ models from the grid of accretion disk models. We then chose the lowest χ^2 model (best fit) and obtain as output the WD temperature (or the mass accretion rate) and the distance to the system. Since the reddening is also not known accurately, the choice $M = 0.9\ M_\odot$ helps us limit the number of solutions to a single table.

4. RESULTS AND DISCUSSION

We first tried a single white dwarf model, then an accretion disk alone, and then a combination of both for the *FUSE* spectrum alone, then for the *HST* STIS spectrum alone, and then for the combined *FUSE* + *HST* STIS spectrum. We note that if we do not deredden the observed spectra, they are basically impossible to fit with our synthetic spectral models.

4.1. *The FUSE Spectrum*

The best solar composition WD model fit we found to the dereddened *FUSE* spectrum of V794 Aql assuming $E(B-V) = 0.1$ has an effective temperature of 44,000 K, a rotation rate of 200 km s^{-1}, and a distance of 301 pc. This model is listed in Table 5. The WD model has some absorption features (around 1120–1130 Å) not present at all in the observed spectrum. In order to try and improve the fit, we decrease the abundances of C and Si (responsible for these absorption features) to 0.01 times their solar value and kept all the other abundances solar. This provides a 10% reduction in the χ^2_ν value (Table 5).

Next we ran the fitting subroutine on the grid of accretion disk models and found that the fit is slightly better for the disk than for the WD. The best-fit accretion disk models are also listed in Table 5 for the $M = 0.8\ M_\odot$ and $M = 1.03\ M_\odot$ cases. The mass accretion rate we obtained is pretty large ($\dot{M} = 10^{-9}$ to $10^{-8.5}\ M_\odot\ \mathrm{yr}^{-1}$), and the distance is much larger than for a WD model, namely, $d = 616$–834 pc. In Figure 4 we show the best-fit accretion disk model with $M = 1.03\ M_\odot$ and $\dot{M} = 10^{-9}\ M_\odot\ \mathrm{yr}^{-1}$. The inclination angle we obtained is 60°. In fact, for all the disk models we found in the present work, the best fit is obtained for the higher inclination. This comes from the fact that the slope of the continuum is better matched by a rather flat continuum, which is obtained naturally with a higher inclination. A flatter continuum can also be obtained by dereddening the spectrum assuming a higher $E(B-V)$ value, which is what we did next.

We ran our fitting subroutine for the WD and accretion disk models assuming now $E(B-V) = 0.2$, and dereddening the *FUSE* spectrum of V794 Aql accordingly. We found that the χ^2_ν value decreases by about 20% for all the models. However, now the best WD model has a temperature of 51,000 K (since the spectrum is now "bluer") and a distance of 200 pc. The best WD model fit assuming low C and Si abundances is presented in Figure 5 (see also Table 5). For the best accretion disk model we found a slightly higher mass accretion rate ($\dot{M} = 10^{-8.5}$ to $10^{-8.0}\ M_\odot\ \mathrm{yr}^{-1}$) than for the $E(B-V) = 0.1$ case, and a distance $d = 585$–791 pc. Here again the best fit is for the accretion disk models. The 1.03 $M_\odot$ model (Fig. 6) is only marginally better than the 0.8 $M_\odot$ model (all the models are listed in Table 5).

Next we ran two-component (disk+WD) model fits to find whether the fitting can be improved, but we found that the least χ^2_ν obtained for the two-component model is never smaller than the least χ^2_ν obtained for the disk alone.

From the *FUSE* spectrum alone, we find that the best-fit model is that of an accretion disk with a high accretion rate, in agreement with the fact that V794 Aql was caught in a rather high state. The distance inferred from the modeling is pretty large, $d \approx 700 \pm 100$ pc, consistent with the assumption of a large

TABLE 5

Model Fits to the Spectrum of V794 Aql

M_{WD} ($M_\odot$)	T_{WD} (1000 K)	log ($\dot{M}$) ($M_\odot$ yr^{-1})	i (deg)	χ^2_ν	d (pc)	WD/Disk	$E(B-V)$	Spectrum	Figure
0.90.....	44	...	...	0.02959	301	WD	0.10	*FUSE*	...
0.90.....	44	...	...	0.02767	304	WD[a]	0.10	*FUSE*	...
0.80.....	...	−8.5	60	0.02651	834	Disk	0.10	*FUSE*	...
1.03.....	...	−9.0	60	0.02584	616	Disk	0.10	*FUSE*	4
0.90.....	51	...	...	0.02355	199	WD	0.20	*FUSE*	...
0.90.....	51	...	...	0.02257	201	WD[a]	0.20	*FUSE*	5
0.80.....	...	−8.0	60	0.02206	791	Disk	0.20	*FUSE*	...
1.03.....	...	−8.5	60	0.02177	585	Disk	0.20	*FUSE*	6
0.90.....	50	...	...	21.65	281	WD	0.10	STIS	...
0.80.....	...	−9.0	60	13.70	420	Disk	0.10	STIS	...
1.03.....	...	−9.5	60	13.25	311	Disk	0.10	STIS	7
0.90.....	55	...	...	13.65	201	WD	0.20	STIS	...
0.80.....	...	−8.0	60	9.63	794	Disk	0.20	STIS	8
1.03.....	...	−8.5	60	9.82	589	Disk	0.20	STIS	...
0.90.....	30	...		10.9	145	WD	0.10	*FUSE*+STIS	...
0.80.....	...	−9.0	60	5.22	451	Disk	0.10	*FUSE*+STIS	...
1.03.....	...	−9.5	60	4.97	333	Disk	0.10	*FUSE*+STIS	...
0.90.....	45	...		4.47	176	WD	0.20	*FUSE*+STIS	...
0.80.....	...	−8.0	60	3.10	791	Disk	0.20	*FUSE*+STIS	9
1.03.....	...	−8.5	60	3.22	585	Disk	0.20	*FUSE*+STIS	...
0.80.....	47	−9.5	41	4.52	643	56/44	0.20	*IUE*	10
0.80.....	30	...	...	5.17	244	WD	0.20	*IUE*	...

[a] These WD model fits were slightly improved by decreasing C and Si abundances to 0.01 solar.

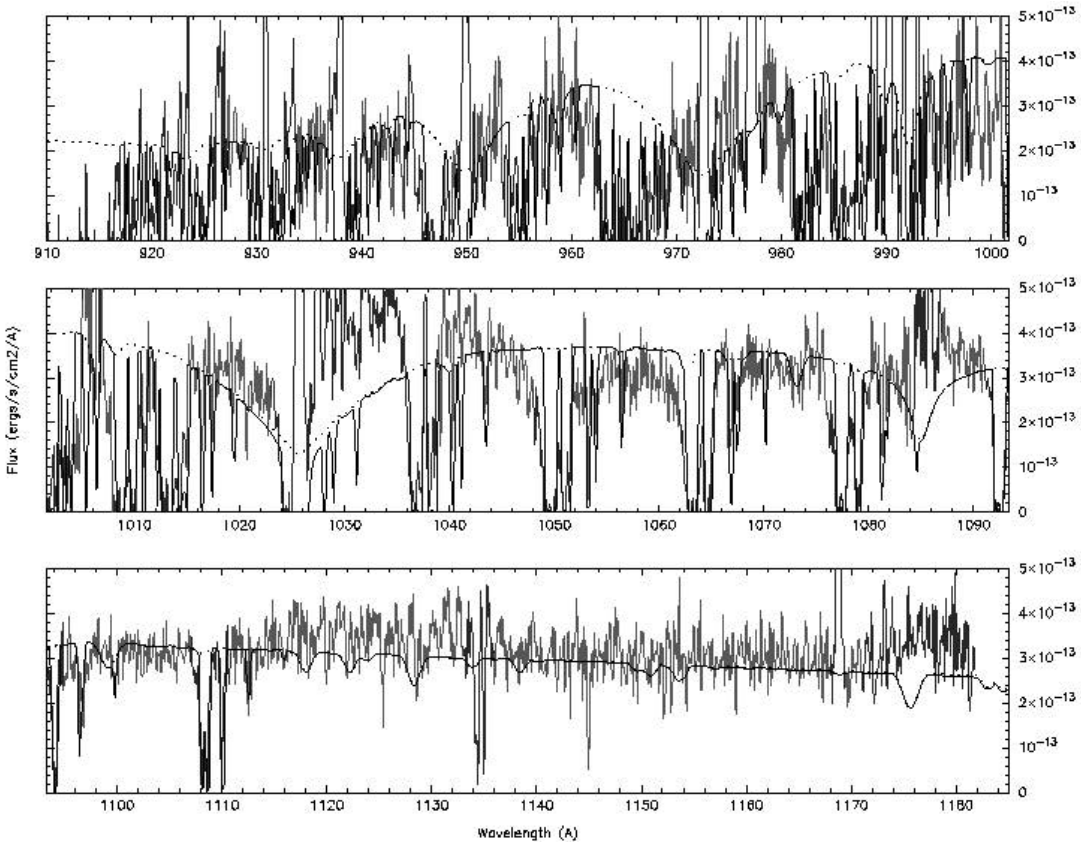

FIG. 5.—Best synthetic spectral fit (*solid black line*) using a WD stellar atmosphere model (with low C and Si abundances) to the dereddened *FUSE* spectrum of V794 Aql assuming $E(B-V) = 0.2$. The WD has a temperature $T_{\rm eff} = 51{,}000$ K, a projected rotation rate of $V_{\rm rot} \sin i = 200$ km s^{-1}, a mass $M = 0.9\,M_\odot$, a distance of 201 pc, and a $\chi^2_\nu = 0.02257$. Note in the synthetic spectrum that the absorption features between 1120 and 1130 Å have been reduced by decreasing the abundances of C and Si to better match the observed spectrum. [*See the electronic edition of the Journal for a color version of this figure.*]

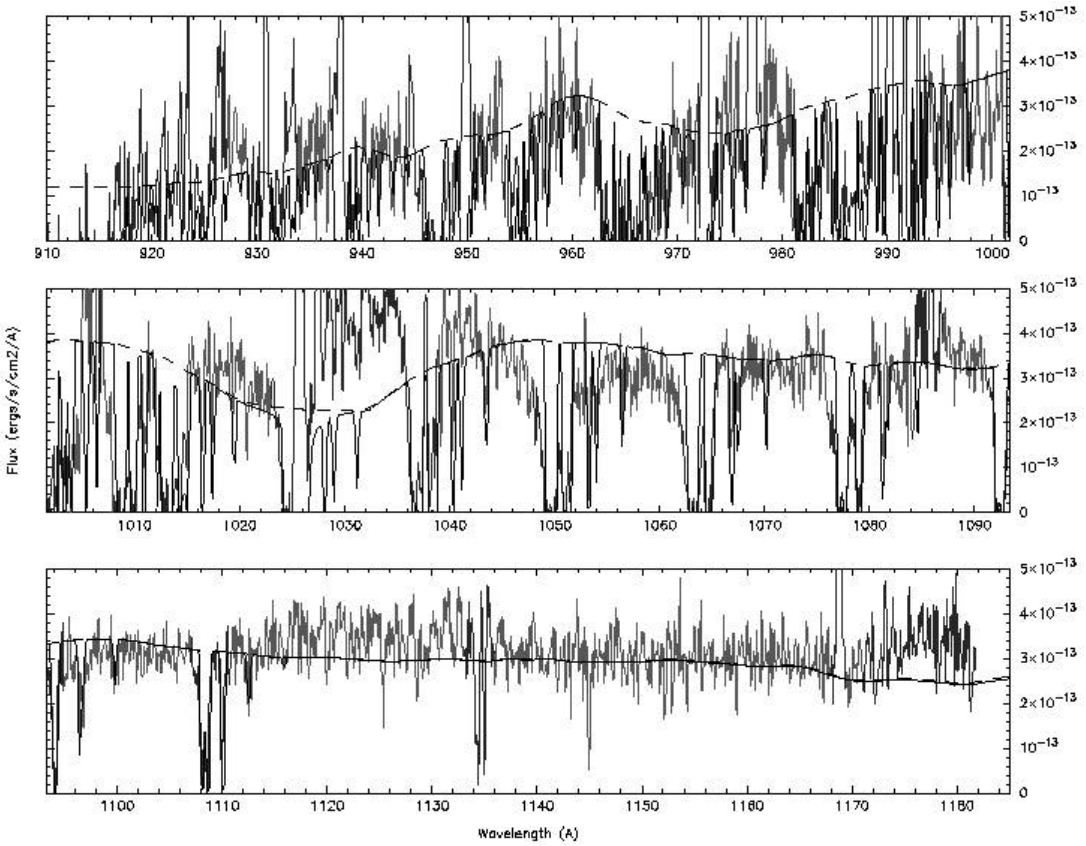

FIG. 6.—Best synthetic spectral fit using a disk model to the dereddened *FUSE* spectrum of V794 Aql assuming $E(B-V)=0.2$. The best fit is for a WD with a mass $M=1.03\,M_{\odot}$, a mass accretion rate is $\dot{M}=10^{-8.5}\,M_{\odot}\,\mathrm{yr}^{-1}$, an inclination of $i=60^{\circ}$, and a distance of 585 pc. The resulting reduced χ^2 is $\chi^2_{\nu}=0.02177$. [*See the electronic edition of the Journal for a color version of this figure.*]

reddening value (0.2) and with the rather low *FUSE* flux for a high state.

4.2. *The HST STIS Spectrum*

Next we carried out exactly the same analysis, but for the *HST* STIS spectrum of V794 Aql, assuming both $E(B-V)=0.1$ and $E(B-V)=0.2$. For easy comparison all these results are also listed in Table 5. The main difference with the *FUSE* results is that the temperature of the best WD model is 6000 K higher for the $E(B-V)=0.1$ case and 4000 K higher for the $E(B-V)=0.2$ case. The distance for the WD models is about the same, namely, $d=200$–300 pc. For the $E(B-V)=0.1$ case, the best accretion disk model (Fig. 7) has a slightly smaller mass accretion rate ($\dot{M}=10^{-9.0}$ to $10^{-9.5}\,M_{\odot}\,\mathrm{yr}^{-1}$) than for the *FUSE* best fit, which leads to about half the distance obtained for the *FUSE* spectrum with the same reddening value. For the $E(B-V)=0.2$ case we obtained exactly the same best accretion disk solution as for the *FUSE* spectrum. The best-fit accretion disk model [for $E(B-V)=0.2$] is presented in Figure 8. Note that for all the STIS spectral fits the χ^2_{ν} values for the disk models are significantly smaller than for the best WD models, namely, $\chi^2_{\nu}=13.25$ versus 21.65 for the $E(B-V)=0.1$ case, and χ^2_{ν}=9.63 versus 13.65 for the $E(B-V)=0.2$ case. This is an indication that from the STIS spectrum alone, the accretion disk is unambiguously the best model fit, and that $E(B-V)=0.2$ might be the correct

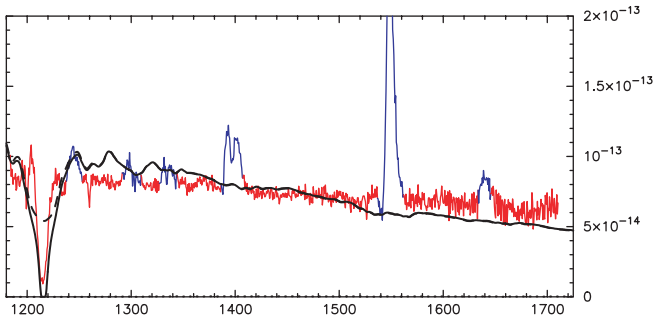

FIG. 7.—Best synthetic spectral fit (*solid black line*) to the dereddened STIS spectrum (*in red and blue*) of V794 Aql assuming $E(B-V)=0.1$. Here too the masked portions are shown in blue and the synthetic spectrum without the ISM model is shown with the dashed line. The best fit consists of an accretion disk model with $\dot{M}=10^{-9.5}\,M_{\odot}\,\mathrm{yr}^{-1}$, around a WD with a mass $M=1.03\,M_{\odot}$, an inclination of $i=60^{\circ}$, and a distance of 311 pc. The resulting reduced χ^2 is $\chi^2_{\nu}=13.25$.

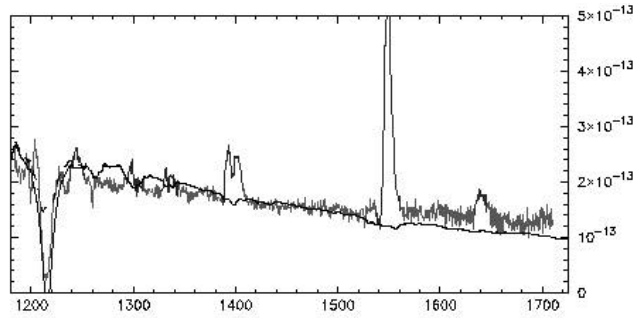

FIG. 8.—Best synthetic spectral fit to the dereddened STIS spectrum of V794 Aql assuming $E(B-V)=0.2$. The best fit consists of an accretion disk model with $\dot{M}=10^{-8.0}\,M_{\odot}\,\mathrm{yr}^{-1}$, around a WD with a mass $M=0.80\,M_{\odot}$, an inclination of $i=60^{\circ}$, and a distance of 794 pc. The resulting reduced χ^2 is $\chi^2_{\nu}=9.63$. [*See the electronic edition of the Journal for a color version of this figure.*]

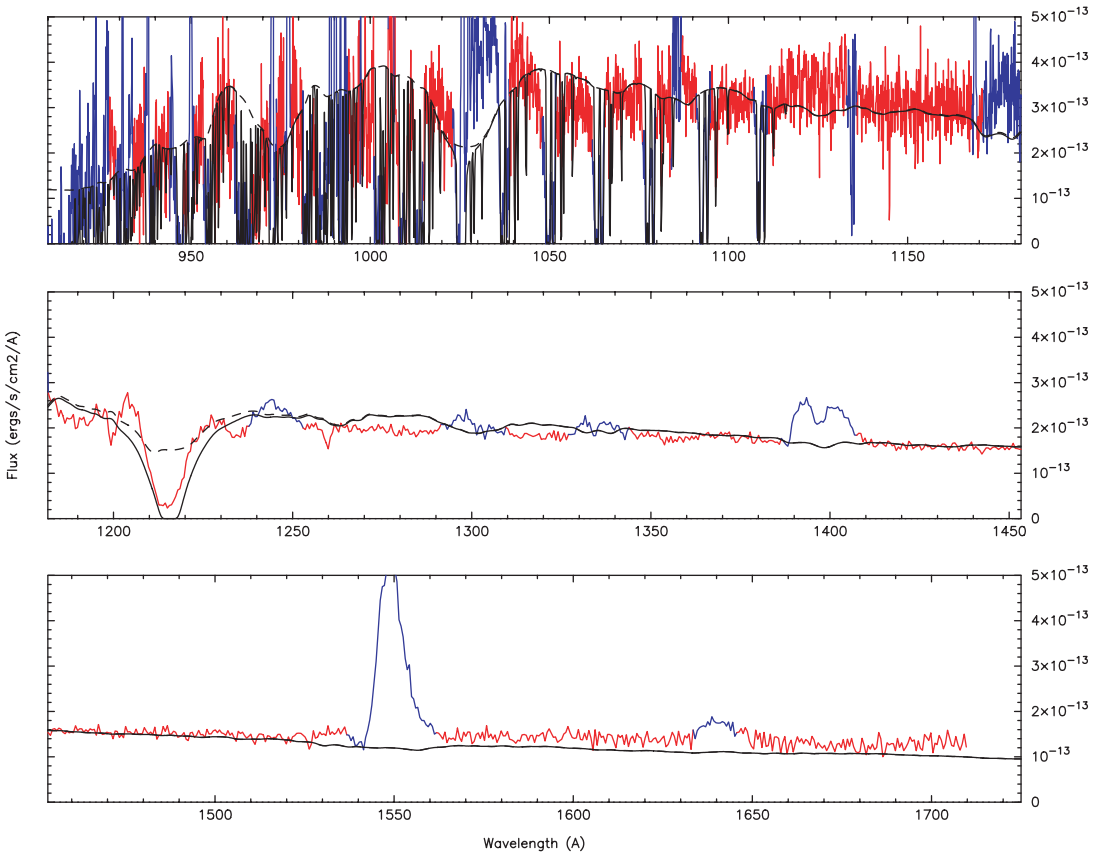

FIG. 9.—Best synthetic spectral fit (*solid black line*) to the dereddened combined (*FUSE*+STIS) spectrum of V794 Aql assuming $E(B-V)=0.2$. The best fit consists of an accretion disk model with $\dot{M}=10^{-8.0}\,M_{\odot}\,\mathrm{yr}^{-1}$, around a WD with a mass $M=0.80\,M_{\odot}$, an inclination of $i=60^{\circ}$, and a distance of 791 pc. The resulting reduced χ^2 is $\chi^2_{\nu}=3.10$.

value for the reddening. Here too the two-component (disk+WD) model did not lead to a better fit.

4.3. *The Combined FUSE + HST STIS Spectrum*

In order to combine the *FUSE* spectrum with the STIS spectrum we check how well their fluxes match in the overlap region between about 1150 and 1180 Å. At very short wavelengths STIS is pretty noisy, and the longer wavelengths of *FUSE* are represented only by one channel (because of the "worm") and are, therefore, less reliable too. Consequently, we are left only with the C III emission region and its immediate vicinity. We find that the spectra have the same flux level there and can therefore be combined together.

Again we ran our fitting subroutine, but now for the combined *FUSE*+STIS spectrum of V794 Aql. This time we found that the temperature for the best WD model fit is much lower than for the individual spectra, namely, 30,000 K for the $E(B-V)=0.1$ case and $T=45{,}000$ K for the $E(B-V)=0.2$ case with a distance of only $d=145$–176 pc. For the $E(B-V)=0.1$ case, we found the same accretion disk solution as for the STIS spectrum, while for the $E(B-V)=0.2$ case (Fig. 9) we found the same accretion disk solution as for the *FUSE* and STIS spectra alone. Again the lowest χ^2_{ν} values were obtained for the accretion disk models. Again the $E(B-V)=0.2$ solutions were better than the $E(B-V)=0.1$ solutions, and here too the two-component (disk+WD) model did not lead to a better fit.

4.4. *The IUE Spectrum in a Low State*

Since the *FUSE* and *HST* STIS spectra were obtained in a relatively high state, we could not get much information on the

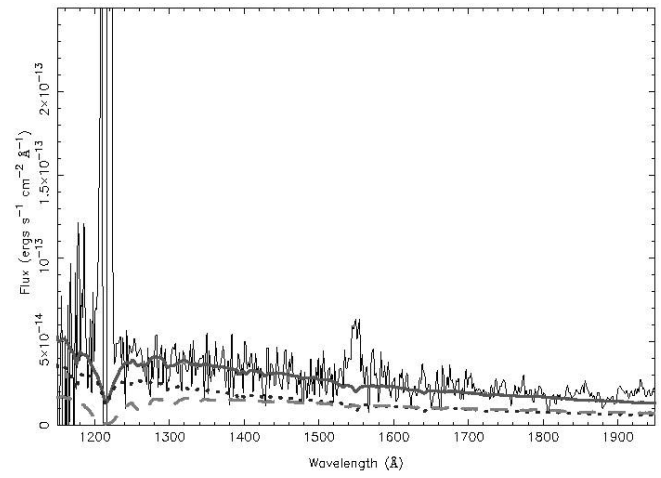

FIG. 10.—Best-fit model (*thick solid line*) to the dereddened *IUE* spectrum SWP 15266 of V794 Aql [assuming $E(B-V)=0.20$] in a relatively low state. The best fit consists of a WD plus an accretion disk model. The WD has a mass $M=0.8\,M_{\odot}$ to agree with the grid of accretion disk models of Wade & Hubeny (1998). The best-fit WD temperature for this model is 47,000 K, the mass accretion rate $\dot{M}=10^{-9.5}\,M_{\odot}\,\mathrm{yr}^{-1}$, the inclination $i=41^{\circ}$, and the distance 643 pc. The resulting reduced χ^2 is $\chi^2_{\nu}=4.52$. In this model the WD (*dotted line*) contributes to 56% of the flux and the disk (*dashed line*) contributes the remaining 44%. [*See the electronic edition of the Journal for a color version of this figure.*]

WD itself. In order to try and gain some knowledge of the WD directly we decided to model the *IUE* spectrum SWP 15266 of V794 Aql in a relatively low state. In this state we expect to see mainly the WD, and therefore we model the spectrum with a $0.8\,M_{\odot}$ WD to agree with the grid of accretion disk models. Since the spectrum is pretty noisy, more than one temperature is obtained, and to limit the number of solutions we fixed the distance to $d \approx 200$ pc and $d \approx 600$ pc and dereddened the spectrum assuming $E(B-V) = 0.20$.

The best-fit model for the shortest distance consists of a WD alone with $T = 30{,}000$ K, with $\chi^2_{\nu} = 5.17$ and a distance of 244 pc.

For the larger distance the best fist consists of a WD plus an accretion disk model (Fig. 10). The WD has $T = 47{,}000$ K, and the disk has $\dot{M} = 10^{-9.5}\,M_{\odot}\ \mathrm{yr}^{-1}$, $i = 41^{\circ}$. This best model has a distance of 643 pc and $\chi^2_{\nu} = 4.52$. In this model the WD contributes 56% of the flux and the accretion disk contributes the remaining 44%. If this temperature is correct, then we have to reject the WD models from Table 5 with $T < 47{,}000$ K for $E(B-V) = 0.20$; this would be the WD model for the combined *FUSE*+STIS spectrum for $[E(B-V) = 0.20]$ with a temperature of only 45,000 K, as this would be inconsistent, namely the system during the higher state cannot have a temperature lower than during quiescence (implying $T > 47{,}000$ K).

5. SUMMARY

We have analyzed the FUV spectra of V794 Aql observed in a relatively high state with *FUSE* and *HST* STIS and found evidence for the presence of a hot accretion disk accreting at a high rate. The spectra exhibit some broad emission lines (O VI, C III, N V, Si IV, C IV, and He II), a clear sign of a hot gas where a high rotational velocity in a disk might be responsible for the broadening of these lines. We were limited in our spectral analysis by the large number of unknown parameters (distance, WD mass, inclination, reddening, WD temperature) and decided to limit the search for a solution assuming $M_{\mathrm{wd}} = 0.9\,M_{\odot}$. For the *FUSE*, STIS, and *FUSE*+STIS spectra of V794 Aql, we found that the accretion disk model provides a better fit to the observed spectra, which is not surprising since the system was observed in a relatively high state when the contribution of the disk is dominant. The best-fit model had a mass accretion rate of $10^{-8.5}$ to $10^{-8.0}\,M_{\odot}\ \mathrm{yr}^{-1}$ and an inclination of 60°, assuming a mass $M = 0.9\,M_{\odot}$. The distance we obtained was $d = 690 \pm 105$ pc and in all the cases the least χ^2_{ν} was obtained for $E(B-V) = 0.2$. We also found that V794 Aql is moderately affected by the ISM with a molecular hydrogen column density of $3 \times 10^{17}\ \mathrm{cm}^{-2}$ and an atomic hydrogen column density of $4.5 \times 10^{20}\ \mathrm{cm}^{-2}$.

We wish to thank the referee for his/her prompt reply and encouraging comments. P. G. wishes to thank the Space Telescope Science Institute for its kind hospitality. This research was partly based on observations made with the NASA-CNES-CSA Far Ultraviolet Spectroscopic Explorer. *FUSE* is operated for NASA by the Johns Hopkins University under NASA contract NAS5-32985. Funding was provided by NASA *FUSE* (Cycle 4) grant NNG04GL45G to Villanova University (P. G.), NASA *FUSE grant* NNG04GC97G to the University of Washington (P. S.), and NASA *FUSE* grant NNG04GL18G (P. E. B.). Additional support for this work was provided by NASA through grant number HST-AR-10657.01-A (*HST* Cycle 14 Archival) to Villanova University (P. G.) and grant number HST-GO-09724 to the University of Washington (P. S.), from the Space Telescope Science Institute, which is operated by the Association of Universities for Research in Astronomy, Incorporated, under NASA contract NAS5-26555.

REFERENCES

Abgrall, H., Roueff, E., & Drira, I. 2000, A&AS, 141, 297
Bohlin, R. C., Savage, B. D., & Drake, J. F. 1978, ApJ, 224, 132
Bruch, A., & Engel, A. 1994, A&AS, 104, 79
Cannizzo, J. K. 1993, ApJ, 419, 318
Gänsicke, B. T., Sion, E. M., Beuermann, K., Fabian, D., Cheng, F., & Krautter, J. 1999, A&A, 347, 178
Godon, P., Sion, E. M., Cheng, F., Szkody, P., Long, K. S., & Froning, C. S. 2004, ApJ, 612, 429
Godon, P., Seward, L, Sion, E. M., & Szkody, P. 2006, AJ, 131, 2634
Hamada, T., & Salpeter, E. E. 1961, ApJ, 134, 683
Hoard, D. W., Linnell, A. P., Szkody, P., Fried, R. E., Sion, E. M., & Wolfe, M. A. 2004, ApJ, 604, 346
Honeycutt, R. K., Cannizzo, J. K., & Robertson, J. W. 1994, ApJ, 425, 835
Honeycutt, R. K., & Robertson, J. W. 1998, AJ, 116, 1961
Honeycutt, R. K., & Schlegel, E. M. 1985, PASP, 97, 1189
Hubeny, I. 1988, Comput. Phys. Commun., 52, 103
Hubeny, I., & Lanz, T. 1995, ApJ, 439, 875
Knigge, C., Long, K. S., Hoard, D. W., Szkody, P., & Dhillon, V. S. 2000, ApJ, 539, L49
La Dous, C. 1991, A&A, 252, 100
Massa, F., & Fitzpatrick, E. 2000, ApJS, 126, 517
Mateo, M., & Szkody, P. 1984, AJ, 89, 863
McCandliss, S. R. 2003, PASP, 115, 651
Morton, D. C. 2000, ApJS, 130, 403
———. 2003, ApJS, 149, 205
Oke, J. B. 1974, ApJS, 27, 21
Press, W. H., Teukolsky, S. A., Vetterling, W. T., Flannery, B. P. 1992, Numerical Recipes in Fortran 77, The Art of Scientific Computing (2nd ed.; Cambridge: Cambridge Univ. Press)
Rana, V. R., Singh, K. P., Barrett, P. E., & Buckley, D. A. H. 2005, ApJ, 625, 351
Shafter, A. W., Cannizzo, J. K., & Waagen, E. O. 2005, PASP, 117, 931
Sion, E. M. 1999, PASP, 111, 532
Sion, E. M., Cheng, F., Godon, P., & Szkody, P. 2007, AJ, submitted
Sion, E. M., Cheng, F., Godon, P., Urban, J., & Szkody, P. 2004, AJ, 128, 1834
Szkody, P., Crosa, L., Bothun, G. D., Downes, R. A., & Schommer, R. A. 1981, ApJ, 249, L61
Szkody, P., Downes, R., & Mateo, M. 1988, PASP, 100, 362
Verbunt, F. 1987, A&AS, 71, 339
Wade, R. A., & Hubeny, I. 1998, ApJ, 509, 350
Warner, B. 1982, Inf. Bull. Var. Stars, 2175, 1
———. 1995, Cataclysmic Variable Stars (Cambridge: Cambridge Univ. Press)
Wood, M. A. 1990, PH. D. thesis, Univ. Texas (Austin)